Link to Leeds Beckett Repository record:
https://eprints.leedsbeckett.ac.uk/id/eprint/9770/

Document Version:
Article (Published Version)

Creative Commons: Attribution 4.0

Search for an Axionlike Particle in *B* Meson Decays

J. P. Lees,[1] V. Poireau,[1] V. Tisserand,[1] E. Grauges,[2] A. Palano,[3] G. Eigen,[4] D. N. Brown,[5] Yu. G. Kolomensky,[5] M. Fritsch,[6] H. Koch,[6] T. Schroeder,[6] R. Cheaib,[7b] C. Hearty,[7a,7b] T. S. Mattison,[7b] J. A. McKenna,[7b] R. Y. So,[7b] V. E. Blinov,[8a,8b,8c] A. R. Buzykaev,[8a] V. P. Druzhinin,[8a,8b] V. B. Golubev,[8a,8b] E. A. Kozyrev,[8a,8b] E. A. Kravchenko,[8a,8b] A. P. Onuchin,[8a,8b,8c,*] S. I. Serednyakov,[8a,8b] Yu. I. Skovpen,[8a,8b] E. P. Solodov,[8a,8b] K. Yu. Todyshev,[8a,8b] A. J. Lankford,[9] B. Dey,[10] J. W. Gary,[10] O. Long,[10] A. M. Eisner,[11] W. S. Lockman,[11] W. Panduro Vazquez,[11] D. S. Chao,[12] C. H. Cheng,[12] B. Echenard,[12] K. T. Flood,[12] D. G. Hitlin,[12] J. Kim,[12] Y. Li,[12] D. X. Lin,[12] S. Middleton,[12] T. S. Miyashita,[12] P. Ongmongkolkul,[12] J. Oyang,[12] F. C. Porter,[12] M. Röhrken,[12] Z. Huard,[13] B. T. Meadows,[13] B. G. Pushpawela,[13] M. D. Sokoloff,[13] L. Sun,[13,†] J. G. Smith,[14] S. R. Wagner,[14] D. Bernard,[15] M. Verderi,[15] D. Bettoni,[16a] C. Bozzi,[16a] R. Calabrese,[16a,16b] G. Cibinetto,[16a,16b] E. Fioravanti,[16a,16b] I. Garzia,[16a,16b] E. Luppi,[16a,16b] V. Santoro,[16a] A. Calcaterra,[17] R. de Sangro,[17] G. Finocchiaro,[17] S. Martellotti,[17] P. Patteri,[17] I. M. Peruzzi,[17] M. Piccolo,[17] M. Rotondo,[17] A. Zallo,[17] S. Passaggio,[18] C. Patrignani,[18,‡] I. Flood,[19] N. Nguyen,[19] B. J. Shuve,[19] H. M. Lacker,[20] B. Bhuyan,[21] U. Mallik,[22] C. Chen,[23] J. Cochran,[23] S. Prell,[23] A. V. Gritsan,[24] N. Arnaud,[25] M. Davier,[25] F. Le Diberder,[25] A. M. Lutz,[25] G. Wormser,[25] D. J. Lange,[26] D. M. Wright,[26] J. P. Coleman,[27] E. Gabathuler,[27,*] D. E. Hutchcroft,[27] D. J. Payne,[27] C. Touramanis,[27] A. J. Bevan,[28] F. Di Lodovico,[28,§] R. Sacco,[28] G. Cowan,[29] Sw. Banerjee,[30] D. N. Brown,[30,‖] C. L. Davis,[30] A. G. Denig,[31] W. Gradl,[31] K. Griessinger,[31] A. Hafner,[31] K. R. Schubert,[31] R. J. Barlow,[32,¶] G. D. Lafferty,[32] R. Cenci,[33] A. Jawahery,[33] D. A. Roberts,[33] R. Cowan,[34] S. H. Robertson,[35a,35b] R. M. Seddon,[35b] N. Neri,[36a] F. Palombo,[36a,36b] L. Cremaldi,[37] R. Godang,[37,**] D. J. Summers,[37,*] P. Taras,[38] G. De Nardo,[39] C. Sciacca,[39] G. Raven,[40] C. P. Jessop,[41] J. M. LoSecco,[41] K. Honscheid,[42] R. Kass,[42] A. Gaz,[43a] M. Margoni,[43a,43b] M. Posocco,[43a] G. Simi,[43a,43b] F. Simonetto,[43a,43b] R. Stroili,[43a,43b] S. Akar,[44] E. Ben-Haim,[44] M. Bomben,[44] G. R. Bonneaud,[44] G. Calderini,[44] J. Chauveau,[44] G. Marchiori,[44] J. Ocariz,[44] M. Biasini,[45a,45b] E. Manoni,[45a] A. Rossi,[45a] G. Batignani,[46a,46b] S. Bettarini,[46a,46b] M. Carpinelli,[46a,46b,††] G. Casarosa,[46a,46b] M. Chrzaszcz,[46a] M. De Nuccio,[46a,46b] F. Forti,[46a,46b] M. A. Giorgi,[46a,46b] A. Lusiani,[46a,46c] B. Oberhof,[46a,46b] E. Paoloni,[46a,46b] M. Rama,[46a] G. Rizzo,[46a,46b] J. J. Walsh,[46a] L. Zani,[46a,46b] A. J. S. Smith,[47] F. Anulli,[48a] R. Faccini,[48a,48b] F. Ferrarotto,[48a] F. Ferroni,[48a,‡‡] A. Pilloni,[48a,48b] G. Piredda,[48a,*] C. Bünger,[49] S. Dittrich,[49] O. Grünberg,[49] M. Heß,[49] T. Leddig,[49] C. Voß,[49] R. Waldi,[49] T. Adye,[50] F. F. Wilson,[50] S. Emery,[51] G. Vasseur,[51] D. Aston,[52] C. Cartaro,[52] M. R. Convery,[52] J. Dorfan,[52] W. Dunwoodie,[52] M. Ebert,[52] R. C. Field,[52] B. G. Fulsom,[52] M. T. Graham,[52] C. Hast,[52] W. R. Innes,[52,*] P. Kim,[52] D. W. G. S. Leith,[52,*] S. Luitz,[52] D. B. MacFarlane,[52] D. R. Muller,[52] H. Neal,[52] B. N. Ratcliff,[52] A. Roodman,[52] M. K. Sullivan,[52] J. Va'vra,[52] W. J. Wisniewski,[52] M. V. Purohit,[53] J. R. Wilson,[53] A. Randle-Conde,[54] S. J. Sekula,[54] H. Ahmed,[55] N. Tasneem,[55] M. Bellis,[56] P. R. Burchat,[56] E. M. T. Puccio,[56] M. S. Alam,[57] J. A. Ernst,[57] R. Gorodeisky,[58] N. Guttman,[58] D. R. Peimer,[58] A. Soffer,[58] S. M. Spanier,[59] J. L. Ritchie,[60] R. F. Schwitters,[60] J. M. Izen,[61] X. C. Lou,[61] F. Bianchi,[62a,62b] F. De Mori,[62a,62b] A. Filippi,[62a] D. Gamba,[62a,62b] L. Lanceri,[63] L. Vitale,[63] F. Martinez-Vidal,[64] A. Oyanguren,[64] J. Albert,[65b] A. Beaulieu,[65b] F. U. Bernlochner,[65b] G. J. King,[65b] R. Kowalewski,[65b] T. Lueck,[65b] C. Miller,[65b] I. M. Nugent,[65b] J. M. Roney,[65b] R. J. Sobie,[65a,65b] T. J. Gershon,[66] P. F. Harrison,[66] T. E. Latham,[66] R. Prepost,[67] and S. L. Wu[67]

(*BABAR* Collaboration)

[1]*Laboratoire d'Annecy-le-Vieux de Physique des Particules (LAPP), Université de Savoie, CNRS/IN2P3, F-74941 Annecy-Le-Vieux, France*
[2]*Universitat de Barcelona, Facultat de Fisica, Departament ECM, E-08028 Barcelona, Spain*
[3]*INFN Sezione di Bari, I-70126 Bari, Italy*
[4]*University of Bergen, Institute of Physics, N-5007 Bergen, Norway*
[5]*Lawrence Berkeley National Laboratory and University of California, Berkeley, California 94720, USA*
[6]*Ruhr Universität Bochum, Institut für Experimentalphysik 1, D-44780 Bochum, Germany*
[7a]*Institute of Particle Physics, Vancouver, British Columbia, Canada V6T 1Z1*
[7b]*University of British Columbia, Vancouver, British Columbia, Canada V6T 1Z1*
[8a]*Budker Institute of Nuclear Physics SB RAS, Novosibirsk 630090, Russia*
[8b]*Novosibirsk State University, Novosibirsk 630090, Russia*
[8c]*Novosibirsk State Technical University, Novosibirsk 630092, Russia*
[9]*University of California at Irvine, Irvine, California 92697, USA*
[10]*University of California at Riverside, Riverside, California 92521, USA*

[11]*University of California at Santa Cruz, Institute for Particle Physics, Santa Cruz, California 95064, USA*

[12]*California Institute of Technology, Pasadena, California 91125, USA*

[13]*University of Cincinnati, Cincinnati, Ohio 45221, USA*

[14]*University of Colorado, Boulder, Colorado 80309, USA*

[15]*Laboratoire Leprince-Ringuet, Ecole Polytechnique, CNRS/IN2P3, F-91128 Palaiseau, France*

[16a]*INFN Sezione di Ferrara, I-44122 Ferrara, Italy*

[16b]*Dipartimento di Fisica e Scienze della Terra, Università di Ferrarab, I-44122 Ferrara, Italy*

[17]*INFN Laboratori Nazionali di Frascati, I-00044 Frascati, Italy*

[18]*INFN Sezione di Genova, I-16146 Genova, Italy*

[19]*Harvey Mudd College, Claremont, California 91711, USA*

[20]*Humboldt-Universität zu Berlin, Institut für Physik, D-12489 Berlin, Germany*

[21]*Indian Institute of Technology Guwahati, Guwahati, Assam, 781 039, India*

[22]*University of Iowa, Iowa City, Iowa 52242, USA*

[23]*Iowa State University, Ames, Iowa 50011, USA*

[24]*Johns Hopkins University, Baltimore, Maryland 21218, USA*

[25]*Université Paris-Saclay, CNRS/IN2P3, IJCLab, F-91405 Orsay, France*

[26]*Lawrence Livermore National Laboratory, Livermore, California 94550, USA*

[27]*University of Liverpool, Liverpool L69 7ZE, United Kingdom*

[28]*Queen Mary, University of London, London E1 4NS, United Kingdom*

[29]*University of London, Royal Holloway and Bedford New College, Egham, Surrey TW20 0EX, United Kingdom*

[30]*University of Louisville, Louisville, Kentucky 40292, USA*

[31]*Johannes Gutenberg-Universität Mainz, Institut für Kernphysik, D-55099 Mainz, Germany*

[32]*University of Manchester, Manchester M13 9PL, United Kingdom*

[33]*University of Maryland, College Park, Maryland 20742, USA*

[34]*Massachusetts Institute of Technology, Laboratory for Nuclear Science, Cambridge, Massachusetts 02139, USA*

[35a]*Institute of Particle Physics, Montréal, Québec, Canada H3A 2T8*

[35b]*McGill University, Montréal, Québec, Canada H3A 2T8*

[36a]*INFN Sezione di Milano, I-20133 Milano, Italy*

[36b]*Dipartimento di Fisica, Università di Milano, I-20133 Milano, Italy*

[37]*University of Mississippi, University, Mississippi 38677, USA*

[38]*Université de Montréal, Physique des Particules, Montréal, Québec, Canada H3C 3J7*

[39]*INFN Sezione di Napoli and Dipartimento di Scienze Fisiche, Università di Napoli Federico II, I-80126 Napoli, Italy*

[40]*NIKHEF, National Institute for Nuclear Physics and High Energy Physics, NL-1009 DB Amsterdam, The Netherlands*

[41]*University of Notre Dame, Notre Dame, Indiana 46556, USA*

[42]*Ohio State University, Columbus, Ohio 43210, USA*

[43a]*INFN Sezione di Padova, I-35131 Padova, Italy*

[43b]*Dipartimento di Fisica, Università di Padova, I-35131 Padova, Italy*

[44]*Laboratoire de Physique Nucléaire et de Hautes Energies, Sorbonne Université,
Paris Diderot Sorbonne Paris Cité, CNRS/IN2P3, F-75252 Paris, France*

[45a]*INFN Sezione di Perugia, I-06123 Perugia, Italy*

[45b]*Dipartimento di Fisica, Università di Perugia, I-06123 Perugia, Italy*

[46a]*INFN Sezione di Pisa, I-56127 Pisa, Italy*

[46b]*Dipartimento di Fisica, Università di Pisa, I-56127 Pisa, Italy*

[46c]*Scuola Normale Superiore di Pisa, I-56127 Pisa, Italy*

[47]*Princeton University, Princeton, New Jersey 08544, USA*

[48a]*INFN Sezione di Roma, I-00185 Roma, Italy*

[48b]*Dipartimento di Fisica, Università di Roma La Sapienza, I-00185 Roma, Italy*

[49]*Universität Rostock, D-18051 Rostock, Germany*

[50]*Rutherford Appleton Laboratory, Chilton, Didcot, Oxon OX11 0QX, United Kingdom*

[51]*IRFU, CEA, Université Paris-Saclay, F-91191 Gif-sur-Yvette, France*

[52]*SLAC National Accelerator Laboratory, Stanford, California 94309 USA*

[53]*University of South Carolina, Columbia, South Carolina 29208, USA*

[54]*Southern Methodist University, Dallas, Texas 75275, USA*

[55]*St. Francis Xavier University, Antigonish, Nova Scotia, Canada B2G 2W5*

[56]*Stanford University, Stanford, California 94305, USA*

[57]*State University of New York, Albany, New York 12222, USA*

[58]*Tel Aviv University, School of Physics and Astronomy, Tel Aviv 69978, Israel*

[59]*University of Tennessee, Knoxville, Tennessee 37996, USA*

[60]*University of Texas at Austin, Austin, Texas 78712, USA*

[61]*University of Texas at Dallas, Richardson, Texas 75083, USA*

[62a]*INFN Sezione di Torino, I-10125 Torino, Italy*
[62b]*Dipartimento di Fisica, Università di Torino, I-10125 Torino, Italy*
[63]*INFN Sezione di Trieste and Dipartimento di Fisica, Università di Trieste, I-34127 Trieste, Italy*
[64]*IFIC, Universitat de Valencia-CSIC, E-46071 Valencia, Spain*
[65a]*Institute of Particle Physics, Victoria, British Columbia, Canada V8W 3P6*
[65b]*University of Victoria, Victoria, British Columbia, Canada V8W 3P6*
[66]*Department of Physics, University of Warwick, Coventry CV4 7AL, United Kingdom*
[67]*University of Wisconsin, Madison, Wisconsin 53706, USA*

Axionlike particles (ALPs) are predicted in many extensions of the standard model, and their masses can naturally be well below the electroweak scale. In the presence of couplings to electroweak bosons, these particles could be emitted in flavor-changing B meson decays. We report herein a search for an ALP, a, in the reaction $B^{\pm} \to K^{\pm}a$, $a \to \gamma\gamma$ using data collected by the *BABAR* experiment at SLAC. No significant signal is observed, and 90% confidence level upper limits on the ALP coupling to electroweak bosons are derived as a function of ALP mass, improving current constraints by several orders of magnitude in the range 0.175 GeV $< m_a < 4.78$ GeV.

The physics of spontaneous symmetry breaking drives much of the phenomenology of the standard model (SM). For instance, the Higgs mechanism gives mass to the fermions and weak gauge bosons of the SM, while the spontaneous breaking of approximate chiral global symmetries gives rise to pseudo-Goldstone bosons, such as the pions. Many extensions of the SM feature anomalous global symmetries whose spontaneous breaking leads to new pseudo-Goldstone bosons known as axionlike particles (ALPs) [1–4]. Such particles are ubiquitous in beyond-the-SM theories, such as supersymmetry [5–7], as well as in string theory [8–11]. Potentially, ALPs could resolve several outstanding issues related to the naturalness of SM parameters, such as the strong CP problem [1–4] or the hierarchy problem [12], and they may also serve as mediators to dark sectors [13–16]. Consequently, ALPs have motivated a large number of searches in experimental particle physics and cosmology [17–20].

In the simplest models, ALPs predominantly couple to pairs of SM gauge bosons. While the photon and gluon couplings are already significantly constrained by collider and beam-dump experiments for ALP masses in the MeV–GeV range [21–28], the coupling to $W^{\pm}$ bosons is less explored. This coupling leads to ALP production in flavor-changing neutral-current decays, which can serve as powerful discovery modes. For example, flavor-changing B meson and kaon decays already provide the most stringent bounds on invisibly decaying ALPs over a range of masses [29]. The search presented here is the first for visibly

decaying ALPs produced in B meson decays. Its sensitivity complements existing studies of $K \to \pi\gamma\gamma$ [30–32], which have been conservatively reinterpreted to obtain limits on ALP couplings [29].

In the following, we consider a minimal ALP (a) model with coupling g_{aW} to the $SU(2)_W$ gauge-boson field strengths, $W^b_{\mu\nu}$, and Lagrangian

$$\mathcal{L} = -\frac{g_{aW}}{4} a W^b_{\mu\nu} \tilde{W}^{b\mu\nu}, \tag{1}$$

where $\tilde{W}^{b\mu\nu}$ is the dual field-strength tensor. This coupling leads to the production of ALPs at one loop in the process $B^{\pm} \to K^{\pm}a$, where the ALP is emitted from an internal $W^{\pm}$ boson [29]. Electroweak symmetry breaking and the resulting gauge-boson mixing generates an ALP coupling to a pair of photons, and the branching fraction for $a \to \gamma\gamma$ in this model is nearly 100% for $m_a < m_W$. The same ALP production and decay modes also occur in models with axion couplings to gluons [33,34].

We report herein the first search for an ALP in the reaction $B^{\pm} \to K^{\pm}a$, $a \to \gamma\gamma$ in the range 0.175 GeV $< m_a < m_{B^+} - m_{K^+} \approx 4.78$ GeV, excluding the mass intervals 0.45–0.63 GeV and 0.91–1.01 GeV because of large peaking backgrounds from η and η' mesons, respectively. Note that existing searches already constrain $m_a < 0.1$ GeV in the range of couplings to which our search is sensitive [22–26], while the mass range 0.1 GeV $< m_a < 0.175$ GeV is excluded from our analysis due to large peaking π^0 contributions. The $B^{\pm} \to K^{\pm}a$, $a \to \gamma\gamma$ product branching fraction is measured assuming all signal observed is produced in $B^{\pm} \to K^{\pm}a$ with a decaying promptly. However, the ALP has a decay width $\Gamma_a = g^2_{aW}m^3_a \sin^4\theta_W/64\pi$, where θ_W is the weak mixing angle, and the present search has sensitivity to couplings predicting long-lived ALPs for $m_a < 2.5$ GeV.

We additionally determine the branching fraction for $c\tau_a$ values of 1, 10, and 100 mm in this mass range.

The search is based on a sample of 4.72×10^8 $B\bar{B}$ meson pairs corresponding to 424 fb^{-1} of integrated luminosity collected at the $\Upsilon(4S)$ resonance by the *BABAR* detector at the PEP-II e^+e^- storage ring at the SLAC National Accelerator Laboratory [35]. The *BABAR* detector is described in detail elsewhere [36,37]. A small sample, corresponding to 8% of the total data set, is used to optimize the search strategy and is subsequently discarded.

Signal Monte Carlo (MC) events are simulated using EVTGEN [38], with MC samples generated at 24 masses (from 0.1–4.8 GeV) for promptly decaying ALPs and 16 masses for long-lived ALPs (from 0.1–2.5 GeV). We simulate the following reactions to study the background: $e^+e^- \to e^+e^-(\gamma)$ (BHWIDE [39]), $e^+e^- \to \mu^+\mu^-(\gamma)$, $e^+e^- \to \tau^+\tau^-(\gamma)$ (KK with TAUOLA library [40,41]), continuum $e^+e^- \to q\bar{q}$ with $q = u, d, s,$ and c (JETSET [42]), and $e^+e^- \to B\bar{B}$ (EVTGEN). Each background MC sample is weighted to match the luminosity of the dataset. The detector acceptance and reconstruction efficiencies are estimated with a simulation based on GEANT4 [43].

We reconstruct signal $B^\pm$ candidates by combining a pair of photons with a track identified as a kaon by particle identification algorithms [36]. All other reconstructed tracks and neutral clusters in the event are collectively referred to as the rest of the event (ROE). To suppress backgrounds, we require an energy-substituted mass $m_{\mathrm{ES}} = \sqrt{(s/2 + \vec{p}_i \cdot \vec{p}_B)^2/E_i^2 - p_B^2} > 5.0$ GeV and an energy difference $\Delta E = |\sqrt{s}/2 - E_B^*| < 0.3$ GeV, where $\sqrt{s}$ denotes the center-of-mass (c.m.) energy, $\vec{p}_B$ and E_B are the $B^\pm$ momentum and energy in the lab frame, E_B^* is the $B^\pm$ energy in the c.m. frame, and E_i and $\vec{p}_i$ are the energy and momentum of the initial state in the lab frame. A kinematic fit is performed on the selected $B^\pm$ candidates, requiring the photon and kaon candidates to originate from the measured beam interaction region, and constraining their total energy and invariant mass to the nominal $B^\pm$ meson mass and measured c.m. beam energy.

Two boosted decision trees (BDTs) [44] are used to further separate signal from each of the main backgrounds: one BDT is trained using continuum MC background events and the other using B^+B^- MC background events. For the signal sample, we combine events from all simulated ALP masses with prompt decays to obtain a uniform distribution in diphoton invariant mass ($m_{\gamma\gamma}$). Each BDT includes the following 13 observables: invariant mass of the ROE; cosine of the angle between two sphericity axes, one computed with the $B^\pm$ constituents and the other with the ROE; second Legendre moment of the ROE, calculated relative to the $B^\pm$ thrust axis; m_{ES} and ΔE; particle identification information for the $K^\pm$; helicity angle of the $K^\pm$, which is the angle between the $K^\pm$ and the $\Upsilon(4S)$ as measured in the $B^\pm$ frame; helicity angle and
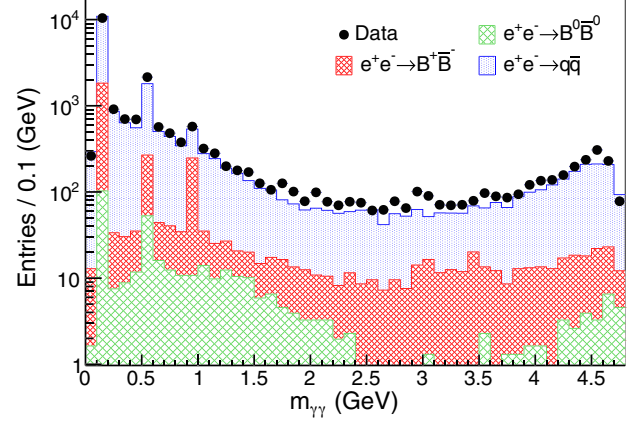

FIG. 1. The diphoton mass distribution of ALP candidates, together with Monte Carlo predictions of leading background processes normalized to the data luminosity.

energy of the most energetic photon forming the a; three invariant masses $m(\gamma_i\gamma_j^P)$, where γ_i is an ALP-daughter photon, γ_j^P is a photon in the ROE, and γ_i and γ_j^P are chosen so that $m(\gamma_i\gamma_j^P)$ is closest to the nominal mass of each of $P = \pi^0, \eta, \eta'$; and, multiplicity of neutral candidates in the event.

The BDT score distributions for data, signal MC, and background MC are provided in the Supplemental Material [45]. For our final signal region selection, we apply the criteria on the two BDT scores shown in Ref. [45], allowing multiple candidates per event. The BDT selection criteria are independent of the ALP mass hypothesis. The signal efficiency estimated from MC varies between 2% for $m_a = 4.78$ GeV to 33% for $m_a = 0.3$ GeV. The resulting $m_{\gamma\gamma}$ distribution is shown in Fig. 1.

The background is dominated by continuum events and by peaking contributions from $B^\pm \to K^\pm h^0$ and $B^\pm \to \pi^\pm h^0$ decays where $h^0 = \pi^0, \eta, \eta'$. The continuum background arises from random combinations of photons and charged hadrons. The observed deviations between MC and data above 1 GeV are due to the challenges of modeling continuum events in this mass range. This is particularly true above 4 GeV where initial-state radiation contributes substantially to the background but is absent from our continuum MC. Over narrow regions of order a few hundred MeV, the data-to-MC ratio is relatively flat for $m_{\gamma\gamma} < 4$ GeV and MC can be used to model the continuum shape in intervals of this width. Nonresonant $B^\pm \to K^\pm\gamma\gamma$ decays and $B^\pm \to K^*\gamma, K^* \to K\gamma$ decays are negligible, as they have total branching fractions $\lesssim 10^{-7}$ [46,47] and do not give a peak in $m_{\gamma\gamma}$. The $B^\pm \to K^\pm\eta_c, \eta_c \to \gamma\gamma$ decay is not included in our background MC; we observe an excess at the η_c mass, with a local significance of 2.6σ as determined by the signal extraction procedure defined below. The measured product branching fraction is consistent with the world average value of $\mathcal{B}(B^\pm \to K^\pm\eta_c)\mathcal{B}(\eta_c \to \gamma\gamma)$ [47]. Because of the relatively small

η_c background compared to the π^0, η, and η', we do not exclude signal mass hypotheses in the vicinity of the η_c mass.

We extract the signal yield of promptly decaying ALPs by performing a series of unbinned maximum likelihood fits of a hypothetical signal peak over a smooth background to the data shown in Fig. 1. We perform fits for 461 signal mass hypotheses with a scan step size equal to the signal resolution, $\sigma_{\gamma\gamma}$. The latter is determined for each simulated ALP mass by fitting the signal sample with a double-sided Crystal Ball function [48], taking the square root of the variance of the Crystal Ball function as $\sigma_{\gamma\gamma}$. We use an interpolating function to determine the value of $\sigma_{\gamma\gamma}$ at intermediate ALP masses. The resolution ranges from 8 MeV near $m_a = 0.175$ GeV to 14 MeV near $m_a = 2$ GeV, and decreasing back to 2 MeV near $m_a = 4.78$ GeV as a result of the constraint imposed on the mass of the $B^\pm$ meson candidate in the kinematic fit. The MC predictions are validated using a sample of $B^\pm \to K^\pm \pi^0$ and $B^\pm \to K^\pm \eta$ decays. The simulated π^0 and η mass resolutions agree with the data to within 3%.

Each unbinned likelihood fit is performed over an $m_{\gamma\gamma}$ interval with a width in the range $(24$–$60)\sigma_{\gamma\gamma}$. The mass-dependent interval width is chosen to be sufficiently broad as to fix the continuum background shape. We have verified that our results are independent of minor variations of the fit interval widths. The probability density function (pdf) includes contributions from signal, continuum background components, and, where needed, peaking components describing the π^0, η, η', and η_c.

The signal pdf is described by a nonparametric kernel density function modeled from signal MC and extrapolated between adjacent simulated mass points [49]. The continuum background is modeled for $m_a < 4$ GeV by the sum of a template derived from smoothed background MC histograms and a first-order polynomial, with the normalization determined from the fit. At higher masses, only the first-order polynomial is needed to model the background. The data-to-MC ratio is approximately constant over each fit interval, and the residual differences are accommodated by the linear polynomial. The shapes of the π^0, η, and η' resonances are also modeled from background MC, while the η_c is modeled using the signal MC mass distribution with a width broadened to match the η_c natural linewidth. For the π^0, η, and η' background components, the normalization is determined from the fit to data, while the normalization of the η_c component is fixed to the product of the world-average value of $\mathcal{B}(B^\pm \to K^\pm \eta_c)\mathcal{B}(\eta_c \to \gamma\gamma)$ and the signal efficiency evaluated at this mass. This allows us to measure an ALP signal rate for $m_a \approx m_{\eta_c}$ while simultaneously accounting for events from $B^\pm \to K^\pm \eta_c, \eta_c \to \gamma\gamma$ decays. We have verified that our signal extraction procedure is robust against changes in the background model by varying the order of the polynomial component of the continuum background.

To assess systematic uncertainties in the MC-derived continuum and peaking background components, we fit the relative normalizations of different background components (continuum $q\bar{q}$, B^+B^-, $B^0\bar{B}^0$) to data rather than fixing each component's normalization to match the luminosity of the total dataset, and we repeat our signal extraction procedure with the reweighted MC-derived templates. We also propagate the uncertainties in the resolution of the peaking components and in the uncertainties in the world-average value of the η_c linewidth. For the η_c model, we assess a systematic uncertainty originating from uncertainties in $\mathcal{B}(B^\pm \to K^\pm \eta_c)\mathcal{B}(\eta_c \to \gamma\gamma)$ by varying the η_c normalization within the uncertainties in the world-average value. The systematic uncertainty in the signal yield resulting from variations in the continuum (peaking) background shape due to refitting the component normalizations is estimated to be, on average, 1% (2%) of the corresponding statistical uncertainty.

We further assess systematic uncertainties associated with our signal model. We derive a systematic uncertainty in the signal yield resulting from our extrapolation of the signal pdf between simulated mass points. We assess this uncertainty by comparing the extracted signal from fits using nearest and next-to-nearest neighbor extrapolation of the signal shape. This uncertainty is estimated to be, on average, 4% of the corresponding statistical uncertainty. We assess a signal resolution systematic uncertainty by repeating our fits with a signal shape whose width is varied within the mass resolution uncertainty, leading to a signal resolution systematic uncertainty that is, on average, 3% of the statistical uncertainty. We determine a systematic uncertainty in the signal efficiency by taking the data/MC ratio for events within 50 MeV of the η' resonance. Events in this interval are predominantly signal-like $B^\pm \to K^\pm \eta', \eta' \to \gamma\gamma$ decays. The data to MC ratio is consistent with unity within statistical errors, and we take the deviation from unity (6%) as a relative systematic uncertainty in the efficiency.

The fitted signal yields and statistical significances are shown in Fig. 2. The largest local significance of 3.3σ is observed near $m_a = 3.53$ GeV with a global significance of 1.1σ after including trial factors [50], consistent with the null hypothesis. Background-only fits to the $m_{\gamma\gamma}$ spectrum are shown over the whole mass range in Ref. [45].

To further validate the signal extraction procedure, we measure the $B^\pm \to K^\pm h^0$, $h^0 \to \gamma\gamma$ ($h^0 = \pi^0, \eta, \eta', \eta_c$) product branching fractions by treating the peaks as signal, extracting the number of events in the peak using the fitting procedure described above, and subtracting nonpeaking background whose magnitude is determined from MC. The results are found to be compatible with the current world averages [47] within uncertainties.

In the absence of significant signal, Bayesian upper limits at 90% confidence level (CL) on $\mathcal{B}(B^\pm \to K^\pm a) \times \mathcal{B}(a \to \gamma\gamma)$ are derived with a uniform positive prior in the product branching fraction. We have verified that the limits

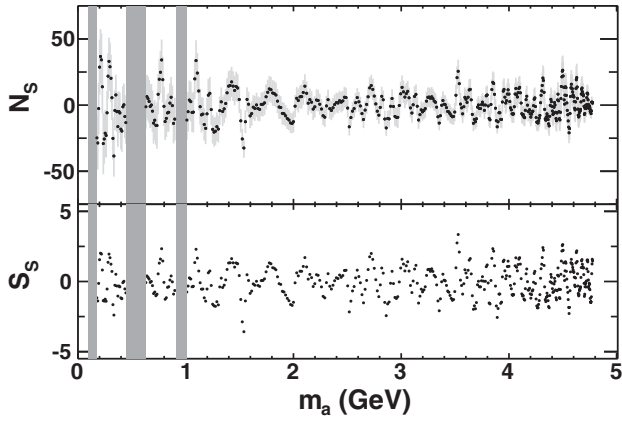FIG. 2. The distribution of signal events (N_s) and local signal significance (S_s) from fits as a function of m_a for prompt ALP decays. The vertical gray bands indicate the regions excluded from the search in the vicinity of the π^0, η, and η' masses.

are robust with respect to the choice of prior. The systematic uncertainty is included in the limit calculation by convolving the likelihood function with a Gaussian having a width equal to the systematic uncertainty. Uncertainties in the luminosity (0.6%) [35] and from the limited statistical precision of simulated samples (1%) are included as well. The resulting limits on the branching fraction product assuming promptly decaying ALPs are displayed in Fig. 3.

Our search targets promptly decaying ALPs. However, ALPs can be long lived at small masses and coupling, and we assess how our signal efficiency and resolution are affected for ALP proper decay lengths of $c\tau_a = 1$, 10, and 100 mm. These decay lengths range from nearly prompt decays for which the efficiency and resolution are comparable to the zero-lifetime signal, through to the longest values to which our analysis is sensitive. We measure the
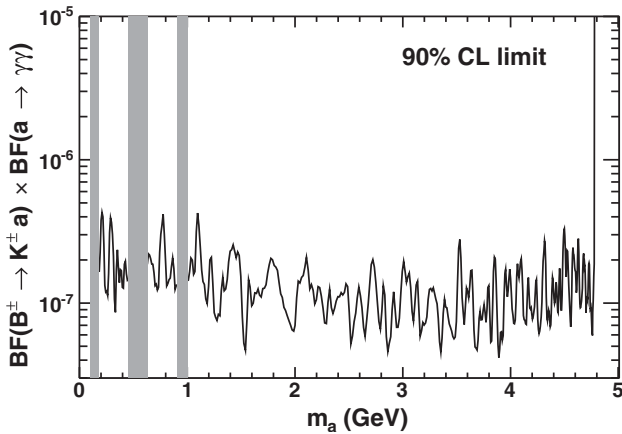
$B^\pm \to K^\pm a$ branching fraction for each decay length. We restrict this study to the mass range for which we obtain sensitivity to couplings that give rise to long-lived ALPs, namely, $m_a < 2.5$ GeV. Long-lived ALPs induce a non-negligible bias in the measurement of $m_{\gamma\gamma}$, and the resolution is significantly impacted, ranging from 15 MeV near $m_a = 0.175$ GeV to 28 MeV near 2 GeV for $c\tau_a = 100$ mm. For $c\tau_a = 100$ mm, we only consider mass hypotheses $m_a \geq 0.2$ GeV, because there is a significant overlap between the signal mass distribution and the π^0 background for lower ALP masses.

The signal is extracted in the same manner as for the promptly decaying ALP, and the fitted signal yields and local statistical significances are shown in Ref. [45]. The largest local significance is found to be at $m_a = 1.10$ GeV and $c\tau_a = 10$ mm, with a global significance of less than one standard deviation. Systematic uncertainties are assessed in the same manner as for the prompt analysis. The systematic uncertainty in the signal yield resulting from variations in the continuum (peaking) background shape due to refitting the component normalizations is larger for long-lived ALPs because of the long tail induced by the bias in the measurement of the signal $m_{\gamma\gamma}$ distribution, and is estimated to be, on average, 16% (24%) of the corresponding statistical uncertainty for $c\tau_a = 100$ mm. The other systematic uncertainties are comparable in magnitude to the values for prompt ALPs, and the total systematic uncertainty is subdominant to the statistical uncertainty for all signal mass hypotheses.

The 90% CL upper limits on $\mathcal{B}(B^\pm \to K^\pm a)\mathcal{B}(a \to \gamma\gamma)$ are plotted in Fig. 4. The limits degrade at $c\tau_a = 100$ mm because of the broadening of the signal shape and lower efficiency. The $c\tau_a$ dependence of the limit is less pronounced at higher masses because the ALP is less boosted, leading to a shorter decay length in the detector. We use an interpolating function to obtain product branching fraction
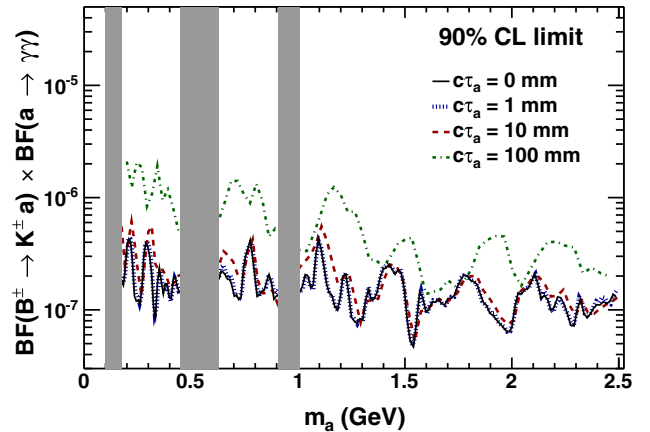

FIG. 3. 90% CL upper limits on the $B^\pm \to K^\pm a$ branching fraction assuming promptly decaying ALPs. The vertical gray bands indicate the regions excluded from the search in the vicinity of the π^0, η, and η' masses.

FIG. 4. The 90% CL upper limits on the $B^\pm \to K^\pm a$ branching fraction for $m_a < 2.5$ GeV and $c\tau_a$ between 0 and 100 mm. The vertical gray bands indicate the regions excluded from the search in the vicinity of the π^0, η, and η' masses.
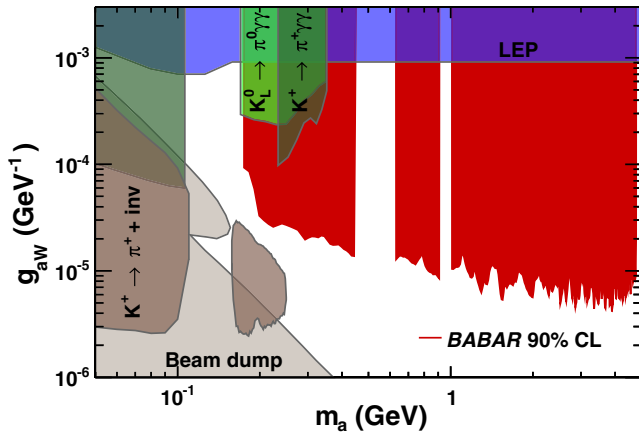
FIG. 5.   The 90% CL upper limits on the coupling g_{aW} as a function of the ALP mass (red), together with existing constraints [29] (blue, green, brown, and gray).

limits for intermediate lifetimes between those shown in Fig. 4.

The 90% CL limits on the ALP coupling g_{aW} are presented in Fig. 5. For each ALP mass hypothesis, we determine the value of g_{aW} such that the calculated branching fraction is equal to the 90%-CL-excluded branching fraction for the lifetime predicted using the same value of g_{aW}. This is the excluded value of g_{aW} shown in Fig. 5. The 90% CL bounds on g_{aW} extend below 10^{-5} GeV^{-1} for many ALP masses, improving current constraints by more than 2 orders of magnitude. The strongest limit on the coupling at $m_a = 0.2$ GeV corresponds to a lifetime of $c\tau_a = 100$ mm, decreasing to $c\tau_a = 1$ mm at $m_a = 2.5$ GeV. Along with our limit, we show in Fig. 5 existing constraints derived in Ref. [29] from LEP, beam dump, and $K \to \pi\gamma\gamma$ searches. We have also reinterpreted a search for $K^{\pm} \to \pi^{\pm}X$ with invisible X [51], which applies to our model if the ALP is sufficiently long lived that it decays outside of the detector.

In summary, we report the first search for axionlike particles in the process $B^{\pm} \to K^{\pm}a$, $a \to \gamma\gamma$. The results strongly constrain ALP couplings to electroweak gauge bosons, improving upon current bounds by several orders of magnitude, except in the vicinity of the π^0, η, and η' resonances. Our results demonstrate the sensitivity of flavor-changing neutral current probes of ALP production, which complement existing searches for the ALP coupling to photons below the B meson mass.

*Deceased.
†Present address: Wuhan University, Wuhan 430072, China.
‡Present address: Università di Bologna and INFN Sezione di Bologna, I-47921 Rimini, Italy.
§Present address: King's College, London WC2R 2LS, United Kingdom.
‖Present address: Western Kentucky University, Bowling Green, Kentucky 42101, USA.
¶Present address: University of Huddersfield, Huddersfield HD1 3DH, United Kingdom.
**Present address: University of South Alabama, Mobile, Alabama 36688, USA.
††Also at: Università di Sassari, I-07100 Sassari, Italy.
‡‡Also at: Gran Sasso Science Institute, I-67100 L'Aquila, Italy.

[1] R. D. Peccei and H. R. Quinn, Phys. Rev. Lett. **38**, 1440 (1977).
[2] R. D. Peccei and H. R. Quinn, Phys. Rev. D **16**, 1791 (1977).
[3] S. Weinberg, Phys. Rev. Lett. **40**, 223 (1978).
[4] F. Wilczek, Phys. Rev. Lett. **40**, 279 (1978).
[5] J. Frere, D. Jones, and S. Raby, Nucl. Phys. **B222**, 11 (1983).
[6] A. E. Nelson and N. Seiberg, Nucl. Phys. **B416**, 46 (1994).
[7] J. Bagger, E. Poppitz, and L. Randall, Nucl. Phys. **B426**, 3 (1994).
[8] E. Witten, Phys. Lett. **149B**, 351 (1984).
[9] J. P. Conlon, J. High Energy Phys. 05 (2006) 078.
[10] P. Svrcek and E. Witten, J. High Energy Phys. 06 (2006) 051.
[11] A. Arvanitaki, S. Dimopoulos, S. Dubovsky, N. Kaloper, and J. March-Russell, Phys. Rev. D **81**, 123530 (2010).
[12] P. W. Graham, D. E. Kaplan, and S. Rajendran, Phys. Rev. Lett. **115**, 221801 (2015).
[13] Y. Nomura and J. Thaler, Phys. Rev. D **79**, 075008 (2009).
[14] M. Freytsis and Z. Ligeti, Phys. Rev. D **83**, 115009 (2011).
[15] M. J. Dolan, F. Kahlhoefer, C. McCabe, and K. Schmidt-Hoberg, J. High Energy Phys. 03 (2015) 171.
[16] Y. Hochberg, E. Kuflik, R. Mcgehee, H. Murayama, and K. Schutz, Phys. Rev. D **98**, 115031 (2018).
[17] R. Essig et al., arXiv:1311.0029.
[18] D. J. E. Marsh, Phys. Rep. **643**, 1 (2016).

[19] P. W. Graham, I. G. Irastorza, S. K. Lamoreaux, A. Lindner, and K. A. van Bibber, Annu. Rev. Nucl. Part. Sci. **65**, 485 (2015).

[20] I. G. Irastorza and J. Redondo, Prog. Part. Nucl. Phys. **102**, 89 (2018).

[21] Throughout, we use natural units with $c = \hbar = 1$ for all energies and masses.

[22] F. Bergsma *et al.* (CHARM Collaboration), Phys. Lett. **157B**, 458 (1985).

[23] E. M. Riordan *et al.*, Phys. Rev. Lett. **59**, 755 (1987).

[24] J. D. Bjorken, S. Ecklund, W. R. Nelson, A. Abashian, C. Church, B. Lu, L. W. Mo, T. A. Nunamaker, and P. Rassmann, Phys. Rev. D **38**, 3375 (1988).

[25] J. Blumlein *et al.*, Z. Phys. C **51**, 341 (1991).

[26] G. Abbiendi *et al.* (OPAL Collaboration), Eur. Phys. J. C **26**, 331 (2003).

[27] D. Aloni, Y. Soreq, and M. Williams, Phys. Rev. Lett. **123**, 031803 (2019).

[28] F. Abudinén *et al.* (Belle II Collaboration), Phys. Rev. Lett. **125**, 161806 (2020).

[29] E. Izaguirre, T. Lin, and B. Shuve, Phys. Rev. Lett. **118**, 111802 (2017).

[30] A. Artamonov *et al.* (E949 Collaboration), Phys. Lett. B **623**, 192 (2005).

[31] E. Abouzaid *et al.* (KTeV Collaboration), Phys. Rev. D **77**, 112004 (2008).

[32] C. Lazzeroni *et al.* (NA62 Collaboration), Phys. Lett. B **732**, 65 (2014).

[33] S. Chakraborty, M. Kraus, V. Loladze, T. Okui, and K. Tobioka, Phys. Rev. D **104**, 055036 (2021).

[34] E. Bertholet, S. Chakraborty, V. Loladze, T. Okui, A. Soffer, and K. Tobioka, arXiv:2108.10331.

[35] J. Lees *et al.* (BABAR Collaboration), Nucl. Instrum. Methods Phys. Res., Sect. A **726**, 203 (2013).

[36] B. Aubert *et al.* (BABAR Collaboration), Nucl. Instrum. Methods Phys. Res., Sect. A **479**, 1 (2002).

[37] B. Aubert *et al.* (BABAR Collaboration), Nucl. Instrum. Methods Phys. Res., Sect. A **729**, 615 (2013).

[38] D. J. Lange, Nucl. Instrum. Methods Phys. Res., Sect. A **462**, 152 (2001).

[39] S. Jadach, W. Placzek, and B. F. L. Ward, Phys. Lett. B **390**, 298 (1997).

[40] S. Jadach, B. F. L. Ward, and Z. Was, Phys. Rev. D **63**, 113009 (2001).

[41] S. Jadach, Z. Was, R. Decker, and J. H. Kuhn, Comput. Phys. Commun. **76**, 361 (1993).

[42] T. Sjöstrand, Comput. Phys. Commun. **82**, 74 (1994).

[43] S. Agostinelli *et al.* (GEANT4 Collaboration), Nucl. Instrum. Methods Phys. Res., Sect. A **506**, 250 (2003).

[44] Y. Freund and R. E. Schapire, J. Comput. Syst. Sci. **55**, 119 (1997).

[45] See Supplemental Material at http://link.aps.org/supplemental/10.1103/PhysRevLett.128.131802 for signal and background distributions of the boosted decision tree classifier scores, example fits of our background model to data, and distributions of extracted signal events and signal significance for long-lived ALPs.

[46] L. Reina, G. Ricciardi, and A. Soni, Phys. Rev. D **56**, 5805 (1997).

[47] P. A. Zyla *et al.* (Particle Data Group), Prog. Theor. Exp. Phys. **2020**, 083C01 (2020).

[48] T. Skwarnicki, Ph. D. Thesis, DESY F31-86-02, Appendix E, 1986.

[49] A. L. Read, Nucl. Instrum. Methods Phys. Res., Sect. A **425**, 357 (1999).

[50] E. Gross and O. Vitells, Eur. Phys. J. C **70**, 525 (2010).

[51] E. Cortina Gil *et al.* (NA62 Collaboration), J. High Energy Phys. 03 (2021) 058.